Virtual MIMO Space Division Multiplexing for MC-CDMA

Koichi Adachi†, Fumiyuki Adachi‡, and Masao Nakagawa†

†Graduate School of Science and Technology, Keio University
3-14-1 Hiyoshi, Kohoku-ku, Yokohama 223-8522, Japan
{kouichi, nakagawa}@nkgw.ics.keio.ac.jp

‡Graduate School of Engineering, Tohoku University
6-6-05 Aza-Aoba, Aramaki, Aoba-ku, Sendai 980-8579 Japan
adachi@ecei.tohoku.ac.jp

Abstract—**To increase the data rate without signal bandwidth expansion, a combination of MC system with multiple-input multiple-output (MIMO)-space division multiplexing (SDM) is attractive. MIMO-SDM transmission performance is governed by min {N_t, N_r}, where N_t and N_r are the numbers of transmit and receive antennas, respectively. For downlink transmission, many receive antennas cannot be equipped at a mobile station due to space limitation. Therefore, the achievable data rate is limited by the number of receive antennas. In this paper, we propose a virtual MIMO-SDM for multi-carrier-code division multiple access (MC-CDMA) that can use the signals received via different propagation paths as virtual receive antennas. The equivalent number of receive antennas can be increased by a factor of the number of distinct paths of the channel. We confirm, by computer simulation, the effectiveness of virtual MIMO-SDM in a frequency-selective fading channel.**

Keywords-component; MIMO; MC-CDMA; Phase rotation

I. INTRODUCTION

Because of the rapid growth of multimedia services, very high speed data transmission is required for the future wireless communication systems [1]. For high speed data transmissions, the wireless channel consists of a number of propagation paths [2] and the channel becomes a severe frequency-selective fading channel. Multi-carrier (MC) system, such as orthogonal frequency division multiplexing (OFDM) and multi-carrier-code division multiple access (MC-CDMA), is robust against the frequency selective fading. To increase the data rate without signal bandwidth expansion, multiple-output (MIMO)-space division multiplexing (SDM) is attractive [3][4]. MIMO-SDM transmission performance is governed by min{N_t, N_r}, where N_t and N_r are the numbers of transmit and receive antennas, respectively [5]. For downlink transmission, many receive antennas cannot be equipped at a mobile station due to space limitation. Therefore, the achievable data rate is limited by the number of receive antennas.

In this paper, we propose a virtual MIMO-SDM for MC-CDMA that can use the signals received via different propagation paths as virtual receive antennas. By removing the phase rotation associated with time delay of each path, the signals received via different propagation paths can be separated through the despreading process without inter-path interference (IPI) to form an N_t-by-$(N_r \cdot L)$ MIMO channel, where L denotes the number of propagation paths. Various MIMO signal detection schemes can be applied to virtual MIMO-SDM. They are maximum likelihood detection (MLD) [6], minimum mean square error (MMSE) detection [7], vertical-Bell laboratory's layered space-time (V-BLAST) detection [8], sphere decoding [9], and QR-decomposition based M-algorithm [10][11].

The rest of the paper is organized as follows. Sect. II gives the received signal representation for virtual MIMO-SDM for MC-CDMA. Virtual MIMO-SDM signal detection is described in Sect. III. Computer simulation results are presented in Sect. IV. Section V concludes the paper.

II. RECEIVED SIGNAL REPRESENTATION

The transmission system model using N_t transmit antennas and N_r receive antennas is illustrated in Fig. 1. In this paper, the discrete-time signal representation is used. The binary data sequence to be transmitted is serial-to-parallel (S/P) converted to N_t streams, each stream being data-modulated. The n_t-th data-modulated symbol stream ($n_t = 0 \sim (N_t - 1)$) is transmitted from the n_t-th transmit antenna using multicode MC-CDMA. In multicode MC-CDMA with N_c sub-carriers and code multiplexing order U, the u-th ($u = 0 \sim (U-1)$) data symbol sequence $\{d_{n_t,u}(n); n = 0 \sim (\lfloor N_c/SF \rfloor - 1)\}$ is spread by the spreading code $\{c_u(q); q = 0 \sim (SF-1)\}$, where $\lfloor x \rfloor$ is the largest integer smaller than or equal to x and SF is the spreading factor. After spreading, the chip sequence is mapped onto equally spaced SF sub-carriers as shown in Fig. 2.

The k-th subcarrier component $S_{n_t}(k)$ can be expressed as

$$S_{n_t}\left(k = \frac{N_c}{SF} \cdot q + n\right) = \sqrt{\frac{2E_c}{SF \cdot T_c}} \sum_{u=0}^{U-1} d_{n_t,u}(n) c_u(q), \quad (1)$$

where E_c is the signal energy per sample of fast Fourier transform (FFT) and T_c is the FFT sample duration. The same spreading code is reused for all the transmit antennas.

The time-domain MC-CDMA signal to be transmitted from the n_t-th transmit antenna is generated by N_c-point inverse FFT (IFFT) as

$$s_{n_t}(t) = \sum_{k=0}^{N_c-1} S_{n_t}(k) \exp\left(j2\pi \frac{t}{N_c} k\right). \quad (2)$$

After inserting an N_g-sample cyclic prefix (CP) into the guard interval (GI) to avoid inter-block interference (IBI), MC-CDMA signal is transmitted.

978-1-4244-2515-0/09/$25.00 ©2009 IEEE

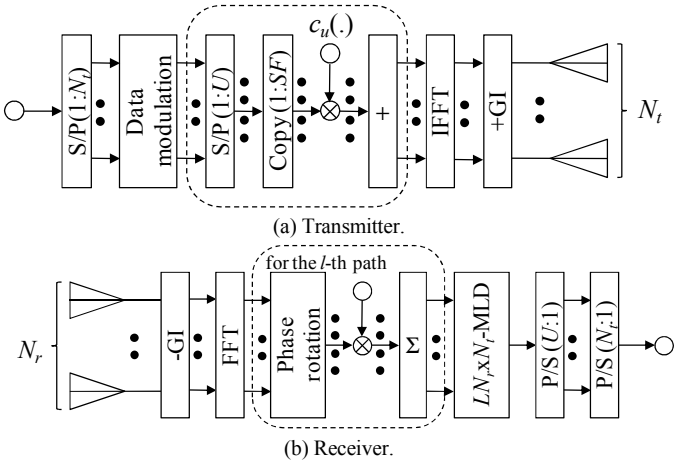

Figure 1. Transmission system model.

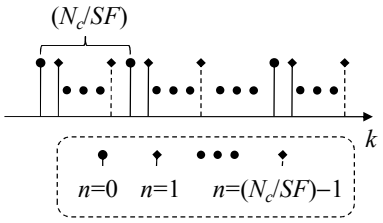

Figure 2. Sub-carrier mapping.

The channel is assumed to be an L-path Rayleigh fading channel with each path time delay being an integer multiple of FFT sample length. The channel impulse response between the n_t-th transmit antenna and the n_r-th receive antenna can be expressed as

$$h_{n_r,n_t}(t)=\sum_{l=0}^{L-1}h_{n_r,n_t,l}\delta(t-\tau_l), \tag{3}$$

where $h_{n_r,n_t,l}$ and τ_l ($\le N_g$) are respectively the complex path gain and the time delay of the l-th path with $E\left[\sum_{l=0}^{L-1}\left|h_{n_r,n_t,l}\right|^2\right]=1$, where $E[.]$ is the ensemble average operation and $\delta(.)$ is the delta function.

The GI-removed received signal $r_{n_r}(t), t=0\sim(N_c-1)$, on the n_r-th receive antenna can be expressed as

$$r_{n_r}(t)=\sum_{n_t=0}^{N_t-1}\sum_{l=0}^{L-1}h_{n_r,n_t,l}s_{n_t}\left((t-\tau_l)\bmod N_c\right)+n_{n_r}(t), \tag{4}$$

where $n_{n_r}(t)$ is the complex-valued additive white Gaussian noise (AWGN) with variance $2\sigma^2=2N_0/T_c$ (N_0 is the single-sided power spectrum density of the AWGN).

The received signal $\{r_{n_r}(t);t=0\sim(N_c-1)\}$ is transformed into frequency-domain signal $\{R_{n_r}(k);k=0\sim(N_c-1)\}$ by N_c-point FFT. $R_{n_r}(k)$ is given by

$$R_{n_r}(k)=\frac{1}{N_c}\sum_{t=0}^{N_c-1}r_{n_r}(t)\exp\left(-j2\pi\frac{k}{N_c}t\right). \tag{5}$$

By substituting (4) into (5), we have

$$R_{n_r}(k)=\sum_{n_t=0}^{N_t-1}H_{n_r,n_t}(k)S_{n_t}(k)+\Pi_{n_r}(k), \tag{6}$$

where $H_{n_r,n_t}(k)$ and $\Pi_{n_r}(k)$ are the Fourier transforms of the impulse response of the channel between the n_t-th transmit antenna and the n_r-th receive antenna and the noise, respectively, and are given by

$$\begin{cases}H_{n_r,n_t}(k)=\sum_{l=0}^{L-1}h_{n_r,n_t,l}\exp\left(-j2\pi\frac{k}{N_c}\tau_l\right)\\ \Pi_{n_r}(k)=\frac{1}{N_c}\sum_{t=0}^{N_c-1}n_{n_r}(t)\exp\left(-j2\pi\frac{k}{N_c}t\right)\end{cases}. \tag{7}$$

III. VIRTUAL MIMO-SDM SIGNAL DETECTION

The virtual MIMO-SDM signal detection consists of two parts: "path separation" and "signal detection".

A. Path Separation

We consider the separation of the l-th path from the received signal. Equation (6) can be rewritten as

$$R_{n_r}(k)=\sum_{n_t=0}^{N_t-1}\left(S_{n_t}(k)\sum_{l'=0}^{L-1}h_{n_r,n_t,l'}\exp\left(-j2\pi\frac{k}{N_c}\tau_{l'}\right)\right)+\Pi_{n_r}(k). \tag{8}$$

The phase rotation in $R_{n_r}(k)$ due to the l-th path time delay is removed as

$$\tilde{R}_{n_r,l}(k)=R_{n_r}(k)\exp\left(j2\pi k\tau_l/N_c\right). \tag{9}$$

By substituting (8) into (9), we have

$$\tilde{R}_{n_r,l}(k)=\sum_{n_t=0}^{N_t-1}\left(S_{n_t}(k)\sum_{l'=0}^{L-1}h_{n_r,n_t,l'}\exp\left(-j2\pi\frac{k}{N_c}(\tau_{l'}-\tau_l)\right)\right)+\Pi_{n_r}(k). \tag{10}$$

Then, frequency domain despreading using the u-th code is performed as

$$\tilde{r}_{u,n_r,l}(n)=(1/SF)\sum_{q=0}^{SF-1}\tilde{R}_{n_r,l}(q\cdot N_c/SF+n)c_u^*(q), \tag{11}$$

which is given as

$$\tilde{r}_{u,n_r,l}(n)=\sum_{n_t=0}^{N_t-1}\left(\sqrt{\frac{2E_c}{SF\cdot T_c}}d_{n_t,u}(n)\times\sum_{l'=0}^{L-1}h_{n_r,n_t,l'}\frac{1}{SF}\sum_{q=0}^{SF-1}\exp\left(-j2\pi\frac{q}{SF}(\tau_{l'}-\tau_l)\right)\right)+\mu_{ICI,u.n_r,l}(n)+\mu_{noise,u,n_r,l}(n). \tag{12}$$

The 1st term is the sum of the signals transmitted from N_t transmit antennas, the 2nd term $\mu_{ICI,u.n_r,l}(n)$ is the inter-code

interference (ICI), and the 3rd term $\mu_{noise,u.n_r,l}(n)$ is the noise component. $\mu_{ICI,u.n_r,l}(n)$ and $\mu_{noise,u.n_r,l}(n)$ are given as

$$\begin{cases} \mu_{ICI,u,n_r,l}(n) \\ = \sqrt{\dfrac{2E_c}{SF \cdot T_c}} \displaystyle\sum_{n_t=0}^{N_t-1} \sum_{\substack{u'=0 \\ \neq u}}^{U-1} \left(d_{n_t,u'}(n) \sum_{l'=0}^{L-1} \left(h_{n_r,n_t,l'} \frac{1}{SF} \sum_{q=0}^{SF-1} X_{u,u',l,l'}(q) \right) \right), \\ \mu_{noise,u,n_r,l}(n) \\ = \dfrac{1}{SF} \displaystyle\sum_{q=0}^{SF-1} \Pi_{n_r}(q) \exp\left(j2\pi \left(\frac{N_c}{SF} \cdot q + n \right) \tau_l \Big/ N_c \right) c_u^*(q) \end{cases} \tag{13}$$

where

$$X_{u,u',l,l'}(q) = c_{u'}(q) c_u^*(q) \exp\left(j2\pi \left(\frac{N_c}{SF} \cdot q + n \right) (\tau_l - \tau_{l'}) \Big/ N_c \right). \tag{14}$$

If the maximum time delay difference among L paths (note that the time delay is normalized by the FFT sample duration) is less than SF, i.e., $\max_{l,l'=0\sim L-1} |\tau_l - \tau_{l'}| \le N_g < SF$, we have

$$\frac{1}{SF} \sum_{q=0}^{SF-1} \exp\left(j2\pi \frac{q}{SF} (\tau_l - \tau_{l'}) \right) = \begin{cases} 1 & \tau_{l'} = \tau_l \\ 0 & \tau_{l'} \ne \tau_l \end{cases}. \tag{15}$$

Substituting (15) into (12), we have

$$\begin{aligned} \tilde{r}_{u,n_r,l}(n) = & \sqrt{\frac{2E_c}{N_c \cdot T_c}} \sum_{n_t=0}^{N_t-1} h_{n_r,n_t,l} d_{n_t,u}(n) \\ & + \mu_{ICI,u,n_r,l}(n) + \mu_{noise,u,n_r,l}(n) \end{aligned}. \tag{16}$$

The signal received via the l-th path is separated without causing IPI.

B. Signal Detection

Through the despreading process explained in Sect. III. A, a total of $(N_r \cdot L)$ received signals are obtained to form the virtual MIMO-SDM received signals. The N_t transmitted and $(N_r \cdot L)$ received signals can be expressed using the matrix form as

$$\tilde{\mathbf{r}}_u(n) = \sqrt{2E_c/(N_c \cdot T_c)} \mathbf{h} \mathbf{d}_u(n) + \boldsymbol{\mu}_{ICI,u}(n) + \boldsymbol{\mu}_{noise,u}(n), \tag{17}$$

where

$$\begin{cases} \tilde{\mathbf{r}}_u(n) = \left(\tilde{r}_{u,0,0}(n) \quad \cdots \quad \tilde{r}_{u,N_r-1,L-1}(n) \right)^T \\ \mathbf{h} = \begin{pmatrix} h_{0,0,0} & \cdots & h_{0,N_t-1,0} \\ \vdots & \ddots & \vdots \\ h_{N_r-1,0,L-1} & \cdots & h_{N_r-1,N_t-1,L-1} \end{pmatrix} \\ \mathbf{d}_u(n) = \left(d_{0,u}(n) \quad \cdots \quad d_{N_t-1,u}(n) \right)^T \\ \boldsymbol{\mu}_{ICI,u}(n) = \left(\mu_{ICI,u,0,0}(n) \quad \cdots \quad \mu_{ICI,u,N_r-1,L-1}(n) \right)^T \\ \boldsymbol{\mu}_{noise,u}(n) = \left(\mu_{noise,u,0,0}(n) \quad \cdots \quad \mu_{noise,u,N_r-1,L-1}(n) \right)^T \end{cases}. \tag{18}$$

TABLE I. NUMERICAL CONDITION

Number of transmit antennas		N_t=4
Number of receive antennas		N_r=1
Number of sub-carriers		N_c=256
Spreading factor		SF=256
GI length		N_g=32
Code multiplexing order		U=1, 16
Spreading code	Short	Walsh Hadamard
	Long	M-sequence
Channel model	Fading	Block Rayleigh fading
	Power delay profile	L-path uniform
	l-th path time delay	l FFT samples
Channel estimation		Ideal
MIMO signal detection		MLD/QRD-M

Various MIMO signal detection methods can be applied to virtual MIMO-SDM signal detection. Below, we apply MLD [6] and MMSE QRD-M [11].

1) MLD

MLD detection which outputs the transmit signal estimate as

$$\begin{aligned} \tilde{\mathbf{d}}_u(n) &= \left(\tilde{d}_{0,u}(n) \quad \cdots \quad \tilde{d}_{N_t-1,u}(n) \right)^T \\ &= \arg\min_{\tilde{\mathbf{d}}_u(n)} \left(\sum_{n_r=0}^{N_r-1} \sum_{l=0}^{L-1} \left| \tilde{r}_{u,n_r,l}(n) - \sqrt{\frac{2E_c}{N_c \cdot T_c}} \sum_{n_t=0}^{N_t-1} h_{n_r,n_t,l} \tilde{d}_{n_t,u}(n) \right|^2 \right). \end{aligned} \tag{19}$$

MLD is the optimal detection, however, it has a very high computational complexity.

2) QRD-M

QRD-M is known as a reduced complexity version of MLD. In QRD-M, QR-decomposition is applied to extended channel matrix $\tilde{\mathbf{h}}$ to decompose $\tilde{\mathbf{h}}$ into unitary matrix $\mathbf{Q}$ ($\mathbf{Q}\mathbf{Q}^H=\mathbf{I}$) and upper triangular matrix $\mathbf{R}$ as

$$\begin{aligned} \tilde{\mathbf{h}} &= \mathbf{Q}\mathbf{R} \\ &= \begin{pmatrix} Q_{0,0,0} & \cdots & Q_{0,N_t-1,0} \\ \vdots & \ddots & \vdots \\ Q_{N_r+N_t-1,0,L-1} & \cdots & Q_{N_r+N_t-1,N_t-1,L-1} \end{pmatrix} \begin{pmatrix} R_{0,0} & \cdots & R_{0,N_t-1} \\ & \ddots & \vdots \\ \mathbf{0} & & R_{N_t-1,N_t-1} \end{pmatrix}, \end{aligned}$$

where $\tilde{\mathbf{h}} = (\mathbf{h}^T \quad \sigma^2 \mathbf{I}_{N_t})^T$.

The extended received signal vector $\hat{\mathbf{r}}_u(n) = (\tilde{\mathbf{r}}_u^T(n) \quad \mathbf{0})^T$ is multiplied by Hermitian transpose of $\mathbf{Q}$ to obtain $\mathbf{y}_u(n)$ as

$$\begin{aligned} \mathbf{y}_u(n) &= \left(y_{u,0}(n) \quad \cdots \quad y_{u,N_t-1}(n) \right)^T \\ &= \mathbf{Q}^H \hat{\mathbf{r}}_u(n) \\ &= \sqrt{\frac{2E_c}{N_c \cdot T_c}} \mathbf{R} \mathbf{d}_u(n) + \mathbf{Q}^H \boldsymbol{\mu}_{ICI,u}(n) + \mathbf{Q}^H \boldsymbol{\mu}_{noise,u}(n) \end{aligned}. \tag{21}$$

Since the signal transmitted from the n_t-th transmit antenna is interfered only by (n_t+1)-th~(N_t-1)-th transmit antennas, signal detection can be efficiently performed using M-algorithm.

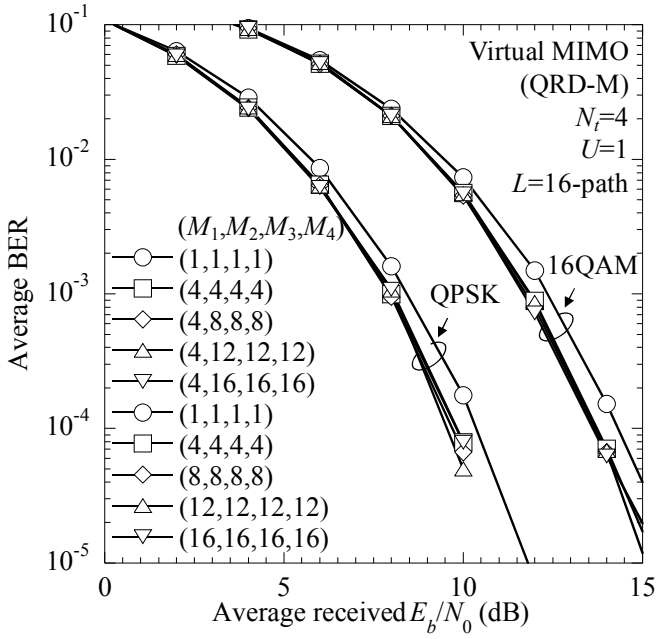

Figure 3. Impact of number of surviving symbol replica candidates.

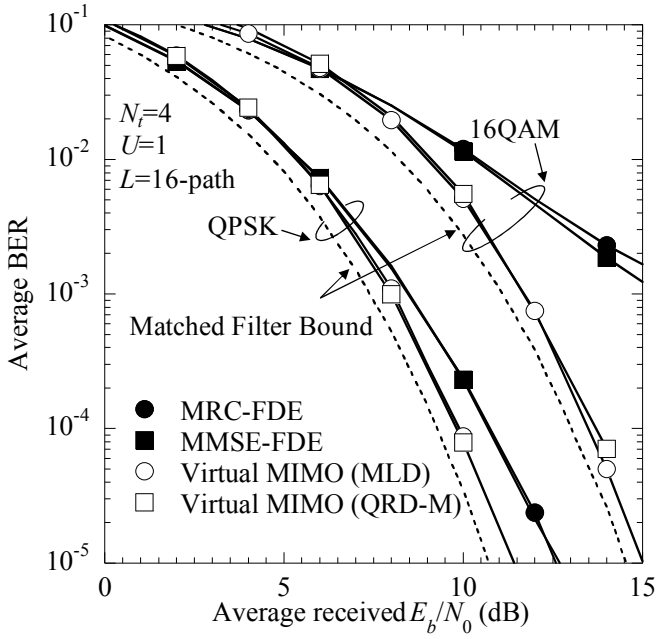

Figure 4. Average BER performance.

IV. Simulation Results

We evaluate the achievable bit error rate (BER) performance of virtual MIMO-SDM and compare it with those of conventional frequency domain equalization using maximum ratio combining (MRC) and minimum mean squared error (MMSE) criteria. The simulation condition is summarized in Table 1. The numbers of transmit and receive antennas are set to N_t=4 and N_r=1, respectively. The number of sub-carriers is set to N_c=256 and the spreading factor is set to SF=256. The GI length is assumed to be N_g=32. QPSK (Quadrature Phase Shift Keying) and 16QAM (Quadrature Amplitude Modulation) are used for data-modulation. The channel between each pair of transmit and receive antennas is assumed to be an independent block Rayleigh fading channel with an L-path uniform power delay profile. The l-th path time delay is assumed to be l FFT samples. At the receiver, ideal channel estimation is assumed. In the virtual MIMO-SDM, the same spreading code, which is a product of Walsh Hadamard (WH) code and a long M-sequence, is reused at all transmit antennas. On the other hand, when the conventional MRC-FDE or MMSE-FDE is used, different spreading codes, each of which is a product of the same WH code and a different M-sequence, are used for N_t transmit antennas.

The average BER performance of the virtual MIMO-SDM using QRD-M is plotted in Fig. 3 as a function of the average received signal energy per bit-to-noise power spectrum density ratio E_b/N_0, where $E_b/N_0=0.5(E_s/N_0)(1+N_g/N_c)$, for U=1 (single-code transmission). In the figure, (M_1,M_2,M_3,M_4) indicate the numbers of surviving symbol replica candidates in the M-algorithm for the signal detection associated with the first, second, third, and fourth transmit antennas, respectively. It can be seen from the figure that the average BER performance of virtual MIMO is not sensitive to the choice of number of surviving symbol replica candidates except for the case of (M_1,M_2,M_3,M_4)=(1,1,1,1). In the following simulation, (M_1,M_2,M_3,M_4)=(4,4,4,4) is used for both QPSK and 16QAM data modulation.

The average BER performance of the virtual MIMO-SDM using MLD and QRD-M is plotted in Fig. 4 as a function of the average received E_b/N_0 when U=1. For comparison, the BER performance is plotted for conventional MRC-FDE and MMSE-FDE having the following FDE weights.

$$w(k)=\begin{cases} H_{0,n_t}^{*}(q) & \text{for MRC} \\ \dfrac{H_{0,n_t}^{*}(q)}{\sum_{n_t=0}^{N_t-1}\left(\dfrac{U}{SF}\cdot\dfrac{E_s}{N_0}\left|H_{0,n_t}(k)\right|^2\right)+1} & \text{for MMSE} \end{cases}. \quad (22)$$

Also plotted in Fig. 4 is the matched filter bound [12]. It can be clearly seen from the figure that the virtual MIMO-SDM can provide better performance than conventional MRC-FDE and MMSE-FDE and achieves the performance close to the matched filter bound. The BER performance loss from the matched filter bound is due to the GI insertion loss of $10\log_{10}(N_c/(N_c+N_g)) \approx 0.51$dB.

Since the virtual MIMO-SDM uses propagation paths as virtual antennas, the achievable BER performance is affected by the number of paths, L. Figure 5 shows the impact of L on the average BER performance of the virtual MIMO-SDM when the average received E_b/N_0=8dB. When L is small, the virtual MIMO-SDM is inferior to the conventional MRC-FDE and MMSE-FDE. This is because, when L is small, the orthogonality among the spreading codes can be almost maintained in the case of conventional FDE. However, L

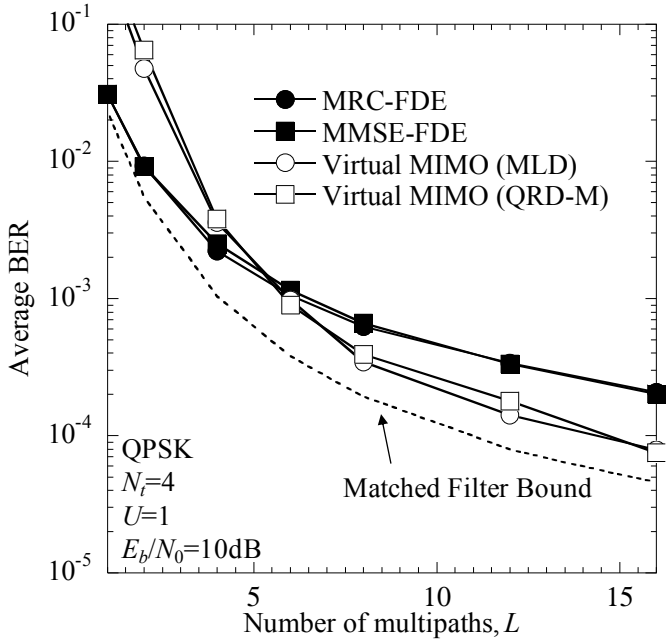

Figure 5. Impact of number of multipaths, L.

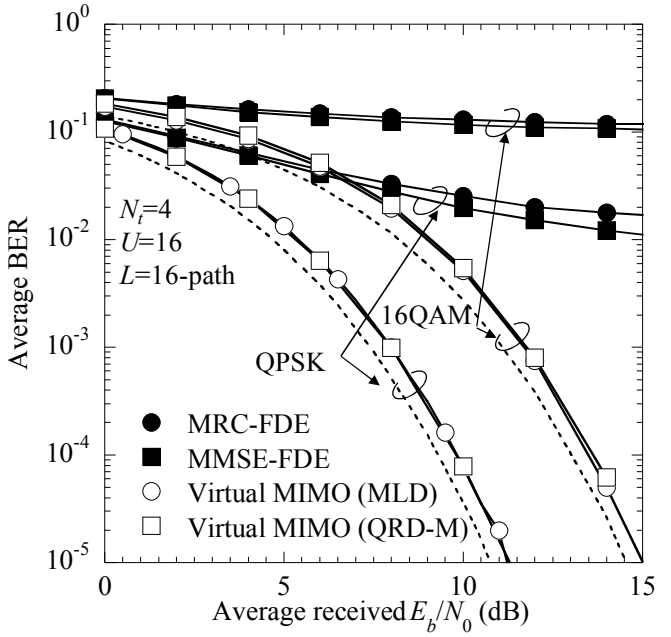

Figure 6. Impact of code multiplexing.

increases beyond 6, the virtual MIMO provides better BER performance than the conventional MRC-FDE and MMSE-FDE.

So far, we have considered U=1 (the single-code transmission), in which increasing the transmission data rate can only be achieved by increasing the number of transmit antennas, N_t. Here, we consider the multi-code transmission (U>1) to further increase the transmission data rate. The average BER performance of the virtual MIMO-SDM is plotted in Fig. 6 for U=16-order code multiplexing per each transmit antenna. The BER performances of conventional MRC-FDE and MMSE-FDE and the matched filter bound are also plotted for comparison. It can be clearly seen that the virtual MIMO-SDM provides much better performance than the conventional MRC-FDE and MMSE-FDE. The effectiveness of the virtual MIMO-SDM is more evident when U>1 than when U=1. The virtual MIMO-SDM using N_t=4 and U=16 provides almost the same BER performance as the single-code/single-transmit antenna case (U=N_t=1) while achieving 64 times higher data rate.

V. Conclusion

In this paper, we proposed a virtual MIMO-SDM for MC-CDMA. In the virtual MIMO-SDM, even if the number of receive antennas is smaller than that of the transmit antennas, the spatial multiplexing gain is not limited by the number of receive antennas. The use of code-multiplexing can further increase the transmission data rate. The average BER performance of the virtual MIMO-SDM was evaluated by computer simulation and compared with those of the conventional MRC-FDE and MMSE-FDE. It was shown that the virtual MIMO-SDM using N_t=4 and U=16 provides almost the same BER performance as the single-code/single-transmit antenna case (U=N_t=1) while achieving 64 times higher data rate.

References

[1] Y. Kim, B. J. Jeong, J. Chung, C. Hwang, J. S. Ryu, K. Kim, and Y. K. Kim, "Beyond 3G: vision, requirements, and enabling technologies," IEEE Commun. Mag., vol.41, pp.120-124, Mar. 2003.

[2] D. Tse and P. Viswanath, Fundamentals of wireless communication, Cambridge University Press, 2005.

[3] G. Stüber, J. Barry, S. Mclaughlin, Y. Li, M. Ingram, and T. Pratt, "Broadband MIMO-OFDM wireless communications," Proc. the IEEE, vol.92, no.2, pp.271-294, Feb. 2004.

[4] M. Juntti, M. Vehkapera, J. Leinonen, V. Zexian, D. Tujkovic, S. Tsumura, and S. Hara, "MIMO MC-CDMA communications for future cellular systems," IEEE Commun., Mag., vol.43, no.2, pp.118-124, Feb. 2005.

[5] L. Zheng and N. C. Tse, "Diversity and multiplexing: A fundamental tradeoff in multiple-antenna channels," IEEE Trans. Inf. Theory, vol.49, no.5, pp.1073-1096, May 2003.

[6] A. van Zelst, R. van Nee, and G. A. Awater, "Space division multiplexing (SDM) for OFDM systems," Proc. IEEE Vehicular Technology Conference (VTC)2000-spring, pp.1070-1074, May 2000.

[7] J. G. Proakis, *Digital Communications*, 4th edition, McGraw-Hill, 2001.

[8] G. J. Foschini, "Layered space-time architecture for wireless communication in a fading environment when using multi-element antennas," Bell Labs Tech. J., vol. 1, no.2, pp.41-59, Aug. 1996.

[9] B. M. Hochwald and S. ten Brink, "Achieving near-capacity on a multiple-antenna channel," IEEE Trans. Commun., vol.51, no.3, pp.389-399, Mar. 2003.

[10] K. J. Kim, J. Yue, R. A. Iltis, and J. D. Gibson, "A QRD-M/Kalman filter-based detection and channel estimation algorithm for MIMO-OFDM systems," IEEE Trans. Wireless Commun., vol.4, no.2, pp.710-721, Mar. 2005.

[11] S. Sun, Y. Dai, Z. Lei, K. Higuchi, and H. Kawai, "Pseudo-inverse MMSE based QRD-M algorithm for MIMO OFDM," Proc. VTC'06-spring, vol.3, pp.1545-1549, May 2006.

[12] F. Adachi and K. Takeda, "Bit error rate analysis of DS-CDMA with joint frequency-domain equalization and antenna diversity combining," IEICE Trans. Commun., vol.E87-B, no.10, pp.2991-3002, Oct. 2004.